Thermal Lattice Parameters Variation of $CaCu_xMn_{7-x}O_{12}$ Compounds with Trigonal Crystal Structure

W. Sławiński[a], R. Przeniosło[a], I. Sosnowska[a],
M. Bieringer[b] and I. Margiolaki[c]

[a]Institute of Experimental Physics, University of Warsaw
Hoża 69, PL-00-681 Warsaw, Poland
[b]Department of Chemistry, University of Manitoba
Winnipeg, Manitoba, R3T 2N2 Canada
[c]European Synchrotron Radiation Facility
BP220, Grenoble Cedex, F-38043, France

We report the crystal structure evolution of $CaCu_{0.2}Mn_{6.8}O_{12}$ as a function of temperature between 10 K and 290 K. The analysis of the diffraction data is carried out with the Rietveld method applied to the average trigonal structure of $CaCu_{0.2}Mn_{6.8}O_{12}$. The $x = 0.2$ member shows similar low temperature extrema for the unit cell parameter evolution as the previously reported $x = 0.1$ and $x = 0$ members of the $CaCu_xMn_{7-x}O_{12}$ system. All magnetic and crystallographic transition temperatures indicated by the unit cell parameter evolution obtained by powder X-ray diffraction methods systematically decrease with increasing Cu content, x.

PACS numbers: 61.05.C–, 65.40.De

1. Introduction

The $CaCu_xMn_{7-x}O_{12}$ family is an important group of manganese oxide systems due to its interesting electronic and magnetic properties such as colossal dielectric responses $CaMn_7O_{12}$ [1] and magnetoresistance observed in e.g. $CaCu_3Mn_4O_{12}$ [2] and $CaCuMn_6O_{12}$ [3]. In agreement with many other manganese oxide systems [4] the $CaCu_xMn_{7-x}O_{12}$ system exhibits an important interplay between magnetic, charge and lattice degrees of freedom.

The undoped $CaMn_7O_{12}$ system has been extensively studied using high resolution neutron diffraction [5–7] and high resolution synchrotron X-ray diffraction [7, 8]. Below 400 K $CaMn_7O_{12}$ crystallises in the trigonal space group $R\bar{3}$ [5, 8]. Below 90 K magnetic long-range ordering with a series of complex magnetic phases and simultaneous magnetic phase separation is observed [6]. Between

90 K and 50 K the coexistence of a ferrimagnetic and a modulated magnetic structure have been reported [6]. At 49 K the ferrimagnetic phase converts into a second modulated magnetic structure. Consequently two modulated magnetic structures with two different magnetic propagation vectors coexist below 49 K [6]. The magnetic phase transition at 49 K coincides with a local maximum of the hexagonal c lattice parameter [7]. The magnetic phase separation in $CaMn_7O_{12}$ has been confirmed by muon spin rotation (μSR) studies since [9].

Below 250 K high resolution synchrotron powder X-ray diffraction patterns show numerous weak Bragg peaks which are forbidden in space group $R\bar{3}$. No corresponding peaks have been observed in powder neutron diffraction experiments, it was therefore concluded that the X-ray satellite peaks are probably due to charge modulation of the manganese ions in the $CaMn_7O_{12}$ structure [10]. The onset of charge ordering is accompanied by a local minimum of the hexagonal c lattice parameter. Furthermore, a structural transition results in a cubic $CaMn_7O_{12}$ high temperature structure (space group: $Im\bar{3}$) above 450 K [8]. Between 410 K and 440 K phase separation causes the trigonal low temperature phase and cubic high temperature phase to coexist as large clusters with domain sizes of at least 150 nm [8]. The phase separation is accompanied by a local maximum of the hexagonal c lattice parameter [8]. The initial observation of phase separation in $CaMn_7O_{12}$ has been recently confirmed by ^{57}Fe Mössbauer studies of $CaMn_{6.97}Fe_{0.03}O_{12}$ [11].

The numerous electronic and magnetic phenomena observed in $CaMn_7O_{12}$ lead to very unusual thermal expansion: the hexagonal lattice parameter has two local maxima and one local minimum as a function of temperature. The main objective of the present paper is to explore the thermal expansion of $CaCu_xMn_{7-x}O_{12}$ compounds with low Cu content, x.

2. Experimental

Polycrystalline powder samples of $CaCu_xMn_{7-x}O_{12}$ for $x = 0.2$ were prepared by annealing stoichiometric amounts of $CaCO_3$ (CERAC, 99.995%), CuO (CERAC, 99.999%), and Mn_2O_3 (CERAC, 99.99%) using KCl as a mineraliser. The synthesis details are described in [12].

Synchrotron radiation powder diffraction measurements were performed on beamline ID31 at the ESRF in Grenoble [13]. The wavelength used was 0.39996 Å. The sample was placed in a 0.5 mm glass capillary which rotated during the experiments. Measurements were performed for the temperatures from 10 K up to 290 K by using a liquid-helium-cooled cryostat. Measurements at temperatures between 290 K and 433 K were performed by using a hot air blower.

The angular range covered by the experiment was $3.5° \leq 2\theta \leq 28.0°$ where 2θ is the scattering angle. The range of the scattering vector Q in the experiment was 0.96 Å$^{-1} \leq Q \leq 7.6$ Å^{-1} and $Q = \frac{4\pi}{\lambda}\sin\theta$.

The SR powder diffraction patterns were analysed by the Rietveld method [14] implemented in the program FullProf [15]. The space group $R\bar{3}$

was used and all atomic positions were refined as well as individual isotropic Debye–Waller factors for each kind of atom. Small amounts of $CaMn_4O_8$ [16] and Mn_2O_3 [17] impurities were identified in the samples.

3. Results

The SR diffraction pattern of $CaCu_{0.2}Mn_{6.8}O_{12}$ at room temperature (RT) cannot be described assuming a pure trigonal phase. Good agreement of the refinement was reached assuming a mixture of about 70% of the trigonal phase and about 30% of a cubic phase contributing to broad peaks as described in [12]. The contribution of the cubic phase of about 20–30% was observed at all temperatures down to 10 K. In this study we describe only the average trigonal crystal structure of $CaCu_{0.2}Mn_{6.8}O_{12}$. During the final refinement cycles all structural parameters including lattice constants, atomic positions and isotropic Debye–Waller factors were refined.
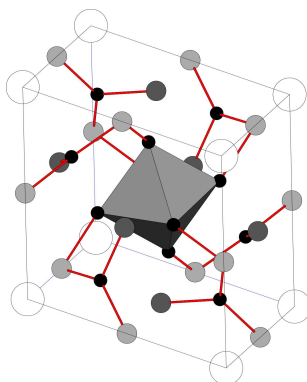
Fig. 1.　(After [12]) Schematic representation of the trigonal $CaCu_xMn_{7-x}O_{12}$ unit cell shown in the rhombohedral setting of space group $R\bar{3}$. White and black circles denote Ca^{2+} and O^{2-} ions, respectively. Dark grey circles denote Mn1 positions occupied by a mixture of Mn and Cu ions. The light grey circles represent Mn ions in Mn2 positions. The central MnO_6 octahedron is regular and centred around the Mn^{4+} ion located in Mn3 position. The network of Mn–O bonds shorter than 2.05 Å is shown with solid lines.

Figure 1 illustrates the crystal structure of $CaCu_xMn_{7-x}O_{12}$ using the commonly used rhombohedral setting. All crystallographic positions are labelled according to Ref. [12]. The distortion of the trigonal unit cell with respect to the cubic unit cell can be conveniently expressed using the angle α_c between two pseudo-cubic cell axes, see e.g. [8], $\cos\alpha_c$ is computed according to

$$\cos\alpha_c = \frac{1 - \frac{3}{8}(a/c)^2}{1 + \frac{3}{4}(a/c)^2}.$$

The complex anisotropic thermal lattice expansion of $CaCu_xMn_{7-x}O_{12}$ phases with $x = 0$, 0.1, and 0.2 are shown in Fig. 2. The temperature dependence of the hexagonal lattice parameters a and c are shown in the upper left and right parts of Fig. 2, respectively. The lower left and right parts in Fig. 2 show the hexagonal unit cell volume and the pseudo-cubic angle α_c, respectively.
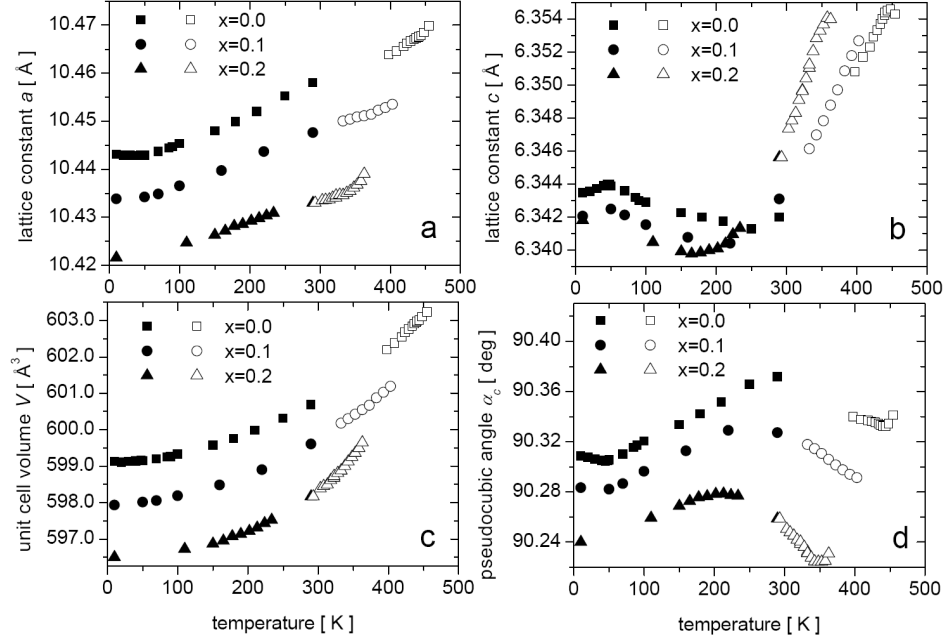
Fig. 2.   Temperature dependence of the hexagonal lattice parameters a (a) and c (b), the unit cell volume (c) and the pseudo-cubic angle α_c (d) of $CaCu_xMn_{7-x}O_{12}$ compounds determined from SR diffraction data by the Rietveld method. $CaMn_7O_{12}$ data (solid squares) are from [10] and (empty squares) — from [8]. $CaCu_{0.1}Mn_{6.9}O_{12}$ data (solid dots) are from [10] and (empty dots) — from [12]. $CaCu_{0.2}Mn_{6.8}O_{12}$ (solid triangles) are present data and (empty triangles) — from [12]. The lattice parameters are given in the hexagonal setting of the trigonal space group $R\bar{3}$.

We are comparing the thermal evolution of $CaCu_{0.2}Mn_{6.8}O_{12}$ for temperatures below room temperature with the previously reported results for $x = 0$ and 0.1. These literature results include: $CaCu_{0.2}Mn_{6.8}O_{12}$ data for temperatures above RT [12], $CaCu_{0.1}Mn_{6.9}O_{12}$ data for temperatures below [10] and above [12] RT, $CaMn_7O_{12}$ data for temperatures below [10] and above [8] RT. Let us note the temperature dependence of all features in Fig. 2 as a function of Cu substitution in $CaCu_xMn_{7-x}O_{12}$. Notably the trigonal to cubic phase transition temperature decreases with increasing Cu content, x.

Let us note that small unit cell parameter discrepancies for $CaMn_7O_{12}$ of recent study [10] with respect to earlier reports on $CaMn_7O_{12}$ prepared by a different synthetic method [7, 8] can be attributed to the use of different peak shape models and application of asymmetry parameters. Despite those numerical deviations the temperature dependences of the lattice parameters are very similar for all reports, thus supporting the validity of diffraction experiments for the investigation of the complex thermal behaviour of the $CaCu_xMn_{7-x}O_{12}$ system.

Figure 2 clearly illustrates the monotonic increase in the hexagonal a axis parameter and the unit cell volume for $CaCu_{0.2}Mn_{6.8}O_{12}$. A similar behaviour is also observed for the $x = 0$ and 0.1 members of the $CaCu_xMn_{7-x}O_{12}$ family (see Fig. 2). Furthermore, the monotonic increase is commonly encountered for many oxide systems. In contrast, the thermal evolution of the hexagonal c lattice parameter and the cubic angle α_c are complex with a possible maximum for the c parameter (and a possible minimum for α_c) between 10 K and 100 K if compared with the $x = 0$ and 0.1 data. In addition, a minimum for the c-axis parameter coinciding with a maximum for α_c are observed above 150 K for $CaCu_{0.2}Mn_{6.8}O_{12}$ again in agreement with corresponding extrema for the $x = 0$ and 0.1 data. The similarities of all three $CaCu_xMn_{7-x}O_{12}$ phases have been clearly identified in this study, suggesting a complex interplay between magnetic, charge and lattice degrees of freedom in the entire $CaCu_xMn_{7-x}O_{12}$ system. We would like to point out that the low temperature diffraction results below 100 K suggest that $CaCu_{0.1}Mn_{6.9}O_{12}$ and $CaCu_{0.2}Mn_{6.8}O_{12}$ may exhibit complex magnetic ordering near 50 K.

4. Conclusions

The low temperature synchrotron powder X-ray diffraction experiments $CaCu_{0.2}Mn_{6.8}O_{12}$ presented in this study revealed unit cell parameter evolutions similar to the remaining members $x = 0$ and 0.1 of the $CaCu_xMn_{7-x}O_{12}$ family. Through comparison with $x = 0$ and 0.1 the experiments indicate the potential for complex magnetic structure evolution below 100 K and similar high temperature charge ordering processes. Notably all the transition temperatures decrease systematically with increasing Cu content in $CaCu_xMn_{7-x}O_{12}$. Additional details regarding the magnetic properties and magnetic structure evolution will be investigated in a future study for a larger range of Cu doping levels in $CaCu_xMn_{7-x}O_{12}$.

Acknowledgments

References

[1] A. Castro-Couceiro, S. Yáñez-Vilar, B. Rivas-Murias, A. Fondado, J. Mira, J. Rivas, M. Señarís-Rodríguez, *J. Phys., Condens. Matter* **18**, 3803 (2006).

[2] Z. Zeng, M. Greenblatt, M.A. Subramanian, M. Croft, *Phys. Rev. Lett.* **82**, 3164 (1999).

[3] D.M. Itkis, E.A. Goodilin, E.A. Pomerantseva, M.V. Lobanov, M. Greenblatt, R. Sivov, J.G. Noudem, Y.D. Tretyakov, *Mendeleev Commun.* **14**, 153 (2004).

[4] E. Dagotto, *Nanoscale Phase Separation and Colossal Magnetoresistance*, Springer, Berlin 2003.

[5] B. Bochu, J.L. Buevoz, J. Chenavas, A. Collomb, J.C. Joubert, M. Marezio, *Solid State Commun.* **36**, 133 (1980).

[6] R. Przeniosło, I. Sosnowska, D. Hohlwein, T. Hauss, I.O. Troyanchuk, *Solid State Commun.* **111**, 687 (1999).

[7] R. Przeniosło, I. Sosnowska, E. Suard, A. Hewat, A.N. Fitch, *Physica B* **344**, 358 (2004).

[8] R. Przeniosło, I Sosnowska, E. Suard, A. Hewat, A.N. Fitch, *J. Phys., Condens. Matter* **14**, 5747 (2002).

[9] A. Prodi, G. Allodi, E. Gilioli, F. Licci, M. Marezio, F. Bolzoni, A. Gauzzi, D. Renzi, *Physica B* **374**, 55 (2006).

[10] W. Sławiński, R. Przeniosło, I. Sosnowska, M. Bieringer, I. Margiolaki, E. Suard, *J. Phys., Condens. Matter* **20**, 104239 (2008).

[11] I.A. Presniakov, V.S. Rusakov, T.V. Gubaidulina, A.V. Sobolev, A.V. Baranov, G. Demazeau, O.S. Volkova, V.M. Cherepanov, E.A. Goodilin, *Solid State Commun.* **142**, 509 (2007).

[12] W. Sławiński, R. Przeniosło, I. Sosnowska, M. Bieringer, I. Margiolaki, A.N. Fitch, E. Suard, *J. Solid State Chem.* **179**, 2443 (2006).

[13] A.N. Fitch, *Res. Natl. Inst. Stand. Technol.* **109**, 133 (2004).

[14] H.M. Rietveld, *J. Appl. Crystallogr.* **2**, 65 (1969).

[15] J. Rodriguez-Carvajal, *Physica B* **192**, 55 (1993).

[16] N. Barrier, C. Michel, A. Maignan, M. Hervieu, B. Raveau, *J. Mater. Chem.* **15**, 386 (2005).

[17] S. Geller, *Acta Crystallogr. B* **27**, 821 (1971).